Journal of Medicinal Chemistry

Article

pubs.acs.org/jmc

Discovery and Characterization of Novel Selective Inhibitors of Carbonic Anhydrase IX

Virginija Dudutienė,[†] Jurgita Matulienė,[†] Alexey Smirnov,[†] David D. Timm,[†] Asta Zubrienė,[†] Lina Baranauskienė,[†] Vaida Morkūnaitė,[†] Joana Smirnovienė,[†] Vilma Michailovienė,[†] Vaida Juozapaitienė,[†] Aurelija Mickevičiūtė,[†] Justina Kazokaitė,[†] Sandra Bakšytė,[†] Aistė Kasiliauskaitė,[†] Jelena Jachno,[†] Jurgita Revuckienė,[†] Miglė Kišonaitė,[†] Vilma Pilipuitytė,[†] Eglė Ivanauskaitė,[†] Goda Milinavičiūtė,[†] Vytautas Smirnovas,[†] Vilma Petrikaitė,[†,∥] Visvaldas Kairys,[‡] Vytautas Petrauskas,[†] Povilas Norvaišas,[†] Darius Lingė,[†] Paulius Gibieža,[†] Edita Čapkauskaitė,[†] Audrius Zakšauskas,[†] Egidijus Kazlauskas,[†] Elena Manakova,[§] Saulius Gražulis,[§] John E. Ladbury,[⊥] and Daumantas Matulis*[,†]

[†]Department of Biothermodynamics and Drug Design, Institute of Biotechnology, [‡]Department of Bioinformatics, Institute of Biotechnology, [§]Department of Protein−DNA Interactions, Institute of Biotechnology, Vilnius University, V. A. Graičiūno 8, Vilnius LT-02241, Lithuania

[∥]Department of Drug Chemistry, Faculty of Pharmacy, Lithuanian University of Health Sciences, A. Mickevičiaus 9, Kaunas LT-44307, Lithuania

[⊥]Department of Biochemistry and Molecular Biology, University of Texas MD Anderson Cancer Center, 1515 Holcombe Boulevard, Houston, Texas 77030, United States

Supporting Information

ABSTRACT: Human carbonic anhydrase IX (CA IX) is highly expressed in tumor tissues, and its selective inhibition provides a potential target for the treatment of numerous cancers. Development of potent, highly selective inhibitors against this target remains an unmet need in anticancer therapeutics. A series of fluorinated benzenesulfonamides with substituents on the benzene ring was designed and synthesized. Several of these exhibited a highly potent and selective inhibition profile against CA IX. Three fluorine atoms significantly increased the affinity by withdrawing electrons and lowering the pK_a of the benzenesulfonamide group. The bulky ortho substituents, such as cyclooctyl or even cyclododecyl groups, fit into the hydrophobic pocket in the active site of CA IX but not CA II, as shown by the compound's co-crystal structure with chimeric CA IX. The strongest inhibitor of recombinant human CA IX's catalytic domain in human cells achieved an affinity of 50 pM. However, the high affinity diminished the selectivity. The most selective compound for CA IX exhibited 10 nM affinity. The compound that showed the best balance between affinity and selectivity bound with 1 nM affinity. The inhibitors described in this work provide the basis for novel anticancer therapeutics targeting CA IX.

		CA IX	CA I
FTSA	K_d	1.1 nM	50,000 nM
ITC	K_d	15 nM	>10,000 nM
SF	K_i	<5.0 nM	46,000 nM

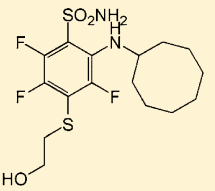

INTRODUCTION

Carbonic anhydrase IX (CA IX) is a transmembrane zinc enzyme that catalyzes the conversion between carbon dioxide and bicarbonate.[1−3] CA IX is considered to be a good tumor marker, as its expression is very limited in normal tissues (almost exclusively expressed in gastrointestinal tract epithelium) and it is highly expressed in various cancers.[4−6] Inhibition of CA IX is a promising therapeutic path for the treatment of solid tumors where a hypoxic environment has developed.[7−9] Hypoxia strongly induces the upregulation of CA IX. As evidenced by in vivo tumor models using gene depletion or overexpression strategies, CA IX is a functional mediator of tumor growth and metastasis.[10−12] CA IX activity is critical for cancer cell survival and adaptation to hypoxic conditions.[13] CA IX also contributes to cancer progression by stimulating cancer cell migration and invasion.[7,12] CA IX activity is also linked to increased tumor resistance to chemo- and radiotherapy, and its inhibition enhances the therapeutic effect of other drugs/radiation.[14−17]

Humans contain 15 highly homologous α-CA isoforms that differ in their oligomeric structure (CAs VI, IX, and XII are dimeric, whereas all other CAs are monomeric), catalytic activity (CAs VIII, X, and XI are catalytically inactive), and cellular localization. CAs I, II, III, VII, and XIII are cytosolic proteins. Catalytic domains of CAs IV, IX, XII, and XIV are on the cell surface; they either are bound to the cell membrane through a GPI anchor (CA IV) or contain a transmembrane domain (CAs IX, XII, and XIV), whereas CAs VA and VB are located in the mitochondrial matrix; CA VI is the only secreted isoform.[2,18,19] The structure of the catalytic domain of human α-CAs is composed of a twisted β-sheet surrounded by α-

Received: July 9, 2014

   dx.doi.org/10.1021/jm501003k | J. Med. Chem. XXXX, XXX, XXX−XXX

Table 1. Compound Dissociation Constants for All 12 Catalytically Active Human CA Isoforms[a]

CA isoform	1 (VD12-09)	2 (PG7)	3 (VD11-4-2)	4 (VD10-13)	5 (VD10-35)	6 (AZM)
			K_d Determined by the Fluorescent Thermal Shift Assay, nM (37 °C, pH 7.0, P_i Buffer)			
CA I	50 000	>200 000	710	0.11	0.20	1400
CA II	1300	>200 000	60	6.7	17	38
CA III	>200 000	>200 000	40 000	29 000	33 000	40 000
CA IV	1700	>200 000	25	590	160	100
CA VA	3300	>200 000	2500	330	290	1000
CA VB	210	>200 000	5.6	1.3	22	310
CA VI	4300	>200 000	95	200	67	310
CA VII	330	>200 000	9.8	46	7.1	17
CA IX	**1.1**	**9.5**	**0.050**	**32**	**50**	**20**
chCA IX	25	630	2.0	63	83	50
CA XII	330	>200 000	3.3	220	250	130
chCA XII	500	>200 000	6.7	310	250	330
CA XIII	140	1700	3.6	8.3	29	50
CA XIV	26	4300	0.16	1.3	5.0	11
			K_d Determined by the Isothermal Titration Calorimetry, nM (37 °C, pH 7.0, P_i or Tris Buffer)			
CA I	>10 000	ND	1100	<10	<10	810
CA II	730	ND	59	<10	<10	46
CA VII	1000	ND	140	59	37	63
CA IX	15	ND	<10	57	51	22
chCA IX	22	ND	7.3	12	14	14
CA XII	230	ND	20	94	140	130
CA XIII	420	ND	42	18	32	60
			K_d by Stopped-Flow Kinetic Inhibition Assay, Fitted by the Morrison eq, nM (25 °C, pH 7.5, Hepes Buffer)			
CA I	46 000	ND	560	<20	ND	290
CA II	910	ND	29	<5.0	ND	10
CA IX	<5.0	ND	<10	25	ND	6.7
chCA IX	15	ND	<5.0	<5.0	ND	<5.0
CA XII	170	ND	<10	110	ND	25
CA XIII	130	ND	<10	<10	ND	<10
			X-ray Crystallographic structure PDB IDs			
CA II	4PYX	ND	4PYY	ND	4PZH	ND
chCA IX	4Q06	ND	4Q07	ND	ND	ND
CA XII	ND	ND	4Q0L	ND	ND	ND
chCA XII	4Q08	ND	4Q09	ND	ND	ND
CA XIII	ND	ND	ND	ND	4HU1	ND

[a]Determined by FTSA, ITC, and stopped-flow kinetic inhibition assays. Available PDB IDs of X-ray crystallographic structures are listed.

helices. All catalytically active human CA isoforms contain a zinc ion at the bottom of their deep active site cleft, which has hydrophobic and hydrophilic surfaces.[20,21] In addition to the catalytic and transmembrane domains and a short intracellular tail, CA IX has a proteoglycan-like domain, a unique feature among other human CA isoforms. Its proposed function is to act as an intrinsic buffer that increases CA IX adaptability to acidic medium.[22]

Currently known CA inhibitors can be divided into two groups: those that coordinate to an active site zinc and those that do not. Among the zinc binders are sulfonamides/sulfamates, ureates/hydroxamates, mercaptophenols, and metal complexing anions.[23] Aromatic sulfonamides are the most widely studied CA inhibitors, with a clearly determined mechanism of inhibition.[24,25] Numerous sulfonamides are being used in the clinic to treat pathologies such as edema, glaucoma, epilepsy, altitude sickness, and others.[23,26] Unfortunately, current inhibitors not only bind to the targeted CA but also to off-target CAs and thus often exhibit undesired side effects.

Here, we describe novel inhibitors that selectively and with subnanomolar affinity bind and inhibit CA IX. The inhibitors are based on fluorinated benzenesulfonamides that have been known to exhibit high affinity toward most CA isoforms.[27−29] We characterized the binding and inhibition characteristics of the inhibitors to all CAs using three complementary techniques: isothermal titration calorimetry (ITC), the fluorescent thermal shift assay (FTSA), and the stopped-flow CO_2 hydration assay. Structural characterization of compound binding was achieved by determining compound co-crystal structures with several selected CA isoforms (CAs I, II, and XII) and several chimeric CAs (chCA IX and chCA XII), which resemble CAs IX and XII. The compounds are good candidates for further development as anticancer agents targeting CA IX.

RESULTS

Binding and Inhibition of CAs. CA IX is a membrane protein containing a proteoglycan-like domain, a transmembrane region, and an intracellular region associated with signaling. The protein dimerizes, exposing the catalytic domain on the cell surface side of the membrane.[1,30,31] The catalytic domain of CA IX was prepared in mammalian cells and purified by affinity chromatography. The measured catalytic activity of CA IX and the inhibition profile by standard inhibitors such as

dx.doi.org/10.1021/jm501003k | J. Med. Chem. XXXX, XXX, XXX−XXX

acetazolamide (**6**, AZM) were similar to those previously published (Table 1).

To design CA IX-selective inhibitors, a series of fluorinated benzenesulfonamides with substituents on the benzene ring was synthesized that was designed to sterically fit in the active site of CA IX but not in the active centers of other CAs. Figure 1 shows the chemical structures of several selected compounds that are described in this study and exhibit subnanomolar affinity and selectivity toward CA IX.

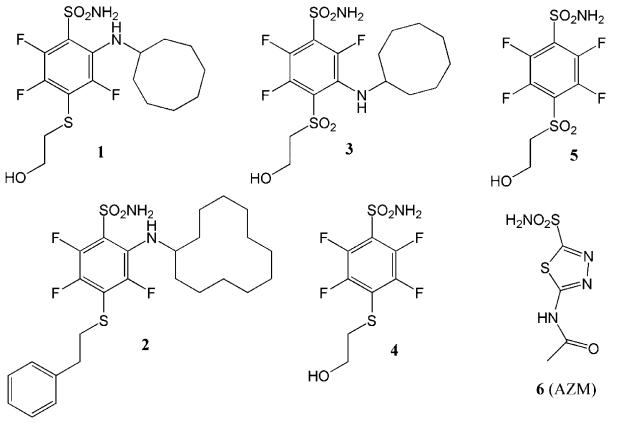

Figure 1. Chemical structures of CA inhibitors discussed in this article. Acetazolamide (**6**, AZM) is commonly used as a control inhibitor of CAs.

The high affinity of the compounds was achieved by lowering the pK_a of the sulfonamide amino group by introducing electron-withdrawing fluorine atoms to the conjugated benzene ring system. Sulfonamide compounds bind and inhibit the CAs in their deprotonated form that is present in a small concentration in the absence of withdrawing groups. In our compounds, a strong withdrawing effect is exhibited by the three fluorine atoms on the benzene ring bound directly to the sulfonamide headgroup.

A large number of techniques have been used to measure inhibitor binding to CAs.[24] The most common current method for determining CA inhibition is the stopped-flow CO_2 hydration inhibition assay.[32−34] However, this method works in the presence of substrate, whereas the direct binding assays are performed in the absence of substrate. ITC,[35−38] surface plasmon resonance (SPR),[39−41] and FTSA[42−46] (often called differential scanning fluorimetry[47] or, in high-throughput, ThermoFluor[48−53]) are frequently used techniques to characterize binding in the absence of substrate.

Inhibitor affinities toward all 12 catalytically active human CA isoforms were measured. Table 1 lists the observed affinities of the compounds toward all 12 catalytically active CA isoforms, as determined by FTSA. For comparison, the values determined by the enzymatic inhibition assay and ITC are shown for the most important isoforms for which selectivity is to be confirmed, namely, CAs I, II, IX, XII, and XIII.

Compound **1** (VD12-09), bearing a bulky cyclooctylamino group at the ortho position to the sulfonamide head, exhibited a dissociation constant of 1.1 nM for CA IX. The remaining 12 catalytically active human CA isoforms bound the compound with significantly lower affinity: CA XIV, 25 times weaker than that of CA IX; CAs XIII, VB, VII, and XII, over 100 times weaker than that of CA IX; CAs II, VA, and VI, over 1000 times weaker than that of CA IX; and CAs I and III, about 100 000 times weaker than that of CA IX. Thus, there is significant selectivity of this compound to bind CA IX over other isoforms. Compound **2** (PG7) bears an even bulkier cyclododecylamino group and thus has quite low solubility. However, the solubility was sufficient to measure its binding to all CA isoforms by FTSA. Again, CA IX exhibited an affinity of approximately 10 nM, whereas almost all CA isoforms did not bind the compound (the K_d was above the detection limit of the FTSA under assay conditions of 200 μM), with the exception of CAs XIII and XIV that bound **2** with submicromolar affinities (Table 1).

If the cyclooctylamino group substituent is instead in the meta position (compound **3** (VD11-4-2), Table 1), then the compound's affinity toward CA IX increased, but it also bound most other isoforms with nanomolar affinity. There was still significant selectivity exhibited toward CA IX, but this was not as profound as that of compounds in the ortho series. Therefore, compounds like **1** may be better suited as drug leads toward CA IX than **3**.

Several compounds missing the second substituent and bearing only the para tail (**4** (VD10-13) and **5** (VD10-35), Figure 1 and Table 1) were very potent binders of CAs. However, they bound CA IX relatively weaker and exhibited essentially no selectivity toward CA IX. These compounds exhibited subnanomolar affinity toward CA I, an undesired effect because CA I activity is deemed to be essential and its inhibition could lead to toxic side effects. In addition, these compounds are tight binders of CA VB.

Crystal Structures of Compounds Bound to CAs Reveal the Basis of Specificity. The PDB codes of the high-resolution X-ray crystallographic structures of CA−compound complexes are listed at the bottom of Table 1. In all 8 crystal structures determined in this work, the compound is bound at the active site of the CA, and the amino group of the sulfonamide is coordinated by the active site zinc atom. The crystal structure of CA XIII with **5** (PDB ID 4HU1) has been previously determined and described.[27] Although we were able to crystallize the compounds of interest (**1**, **3**, and **5**) with CAs II and XII, crystallization of CA IX was elusive. As a result, we adopted an innovative approach to provide structural insight into small molecule binding. We made a chimeric version of CA IX (chCA IX) that was based on using the CA II protein (which we were able to crystallize) but for which the catalytic site was modified to resemble CA IX. Both CAs II and IX have essentially the same protein chain fold in the vicinity of the active site of both proteins. Although the positions of most amino acids are identical, some that are exposed on the active site cleft are different. Therefore, to create a chimera of the actual catalytic site, we made a multiple-residue mutant of CA II that resembles the amino acids of CA IX. This approach is similar to that for the previously designed mimic of CA IX.[54]

To confirm that such chimeric chCA IX could resemble the behavior of actual human CA IX, an additional similar chimeric, chCA XII, was also created. The compound binding comparison between chCA XII and CA XII, and also between chCA XII and CA II, showed that chimeric chCA XII recognized and bound the compounds with similar affinities to that of CA XII, but it was quite different from CA II. For example, compound **3** bound CA XII with 3.3 nM and chCA XII with 6.7 nM affinity. However, CA II bound the compound with 60 nM affinity. Furthermore, compound **4** bound CA XII with 220 nM and chCA XII with 310 nM affinities, but it bound CA II with 6.7 nM affinity. Therefore, the six mutations that

dx.doi.org/10.1021/jm501003k | J. Med. Chem. XXXX, XXX, XXX−XXX

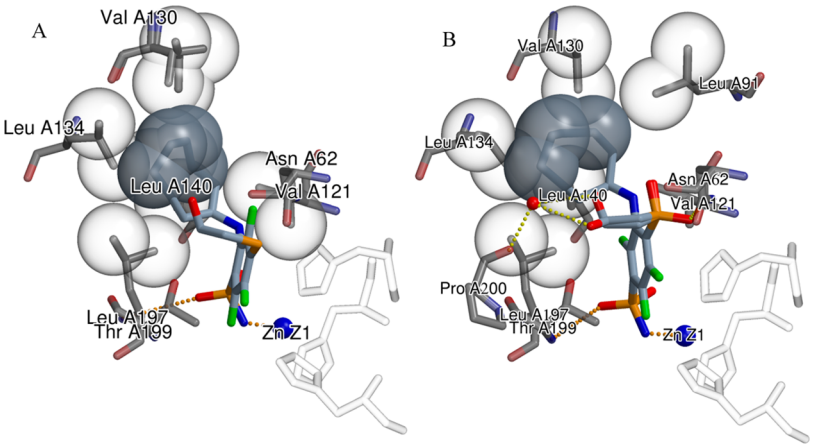

Figure 2. Compounds **1** (A; PDB ID 4Q06) and **3** (B; PDB ID 4Q07) bound to chCA IX, as determined by X-ray crystallography. Zn is shown as a blue sphere, and the histidine residues holding the Zn atom are transparent. The amino acids of chCA IX are shown in gray. The terminal atoms of amino acids that form the hydrophobic cavity are shown as CPK (light gray). Several atoms of the cyclooctyl group are also shown as CPK (dark gray). Dashed lines connect the atoms that make hydrogen bonds or electron donor–acceptor interactions (with Zn). A water molecule is shown as a red sphere. The compounds are shown in light steelblue.

were made to make chCA XII from CA II switched CA II into a CA XII, resembling chCA XII.

Although the chimeric chCA IX shows similar trends in binding data, it does not mimic those of wild-type CA IX to the same extent that chCA XII resembles CA XII. For example, compound **1** bound CA IX with 1.1 nM affinity, whereas it bound chCA IX with 25 nM affinity. Still, this affinity is closer to that of CA IX than to CA II (1300 nM). Compound **4** bound CA II with 6.7 nM affinity, whereas it bound CA IX with 32 nM affinity and chCA IX with 63 nM affinity. Thus, despite the slight variation in binding data between chCA IX and CA IX, we adopted chCA IX to provide structural insight as to how the small molecules are binding.

Figure 2 shows the crystal structures of **1** and **3** bound to chCA IX, emphasizing the nearly perfect filling of the hydrophobic pocket by the cyclooctyl ring and the contacts between the compounds and the protein. Figure 3 compares the structures of **1** and **3** bound to chCA IX, CA II, CA XII, and chCA XII. It is important to understand why compound **1** exhibited such profound selectivity toward CA IX. Figure 3A compares **1** binding to CA II (green) and chCA IX (aquamarine). chCA IX (as well as CA IX, as judged from the only available crystal structure of CA IX in the literature, PDB ID 3IAI) contains a deeper hydrophobic pocket than that of CA II because the bulky Phe131 in CA II occupies part of the pocket. Using this difference between CA II and CA IX, a rather bulky cyclooctyl group has been designed to fit the pocket. This is where it fit in chCA IX, but it could not fit in CA II. Therefore, the ligand adopts the opposite orientation in CA II, and the cyclooctyl group makes poor connections with the protein. Therefore, a ligand such as **1** could be an example of both a tight and selective CA IX-binding compound.

Compound **3**, bearing the cyclooctyl group in the meta position, was less selective toward CA IX than **1** but exhibited some of the highest affinities of any CA inhibitor ever observed, approximately 50 pM. Such affinity could be determined only by FTSA and could not be determined by ITC or the stopped-flow kinetic CO_2 hydration assay because both ITC and the stopped-flow kinetic CO_2 hydration assays are limited by protein concentration. The inhibition assay cannot be performed at lower than 10 nM CA because the signal disappears at these lower protein concentrations. Any ligands that bind tighter to CA than K_d = 10 nM give a nonsymmetrical dosing curve (Figure 4) that simply resembles the titration of 10 nM protein with a ligand that binds significantly tighter than 10 nM affinity. Such nonsymmetrical curves can be fit by using the Morrison equation and should not be fit by a standard Hill equation (see Experimental Section). Due to the above reasons, of the three methods, only the FTSA method could be used to determine the affinity of **3** to CA IX.

Compound **3** bound chCA IX quite similarly to that of **1** (Figure 3B). The overall position of the cyclooctyl group was similar in both structures, but in **3**, the hydrophobic group bound deeper in the pocket, indicating that there was increased contact with the protein.

It would be expected that chimeric CAs exhibit structurally similar binding modes to that of the CAs they were meant to resemble. Compound **3**'s binding mode was determined bound to both CA XII and chCA XII (Figure 3J). Both structures showed a nearly identical binding mode of the compound to actual CA XII and chimeric chCA XII. However, the structure differed from CA II. Therefore, the six mutations introduced to CA II in order to resemble CA XII have switched it into a new protein that is more similar to CA XII than CA II both in terms of its binding affinity and structure.

Interestingly, the structures of both **1** and **3** bound to chCA IX did not contain any water molecules in the vicinity of the active site. All water molecules were efficiently displaced by the ligands. By way of contrast, only para-substituent-bearing compound **5** exhibited average affinity to CA IX (50 nM), but it bound to CA II significantly more tightly (17 nM) and exhibited numerous water molecules in the vicinity of the ligand (Figure 3C). This observation was true both for CA II and CA XIII. Therefore, a bulky ortho or meta substituent is needed to efficiently occupy the space in the active site and displace water molecules. The two bulky hydrophobic groups in compound **2** significantly reduced its water solubility, and no crystal structure was determined for the compound.

Compound **3** bound CA II with 60 nM and CA IX with 50 pM affinities. Thus, there is 1000-fold selectivity toward CA IX. The affinity of the chimeric chCA IX mutant that was used to determine the structure was right in the middle of the range, 2.0

dx.doi.org/10.1021/jm501003k | J. Med. Chem. XXXX, XXX, XXX–XXX

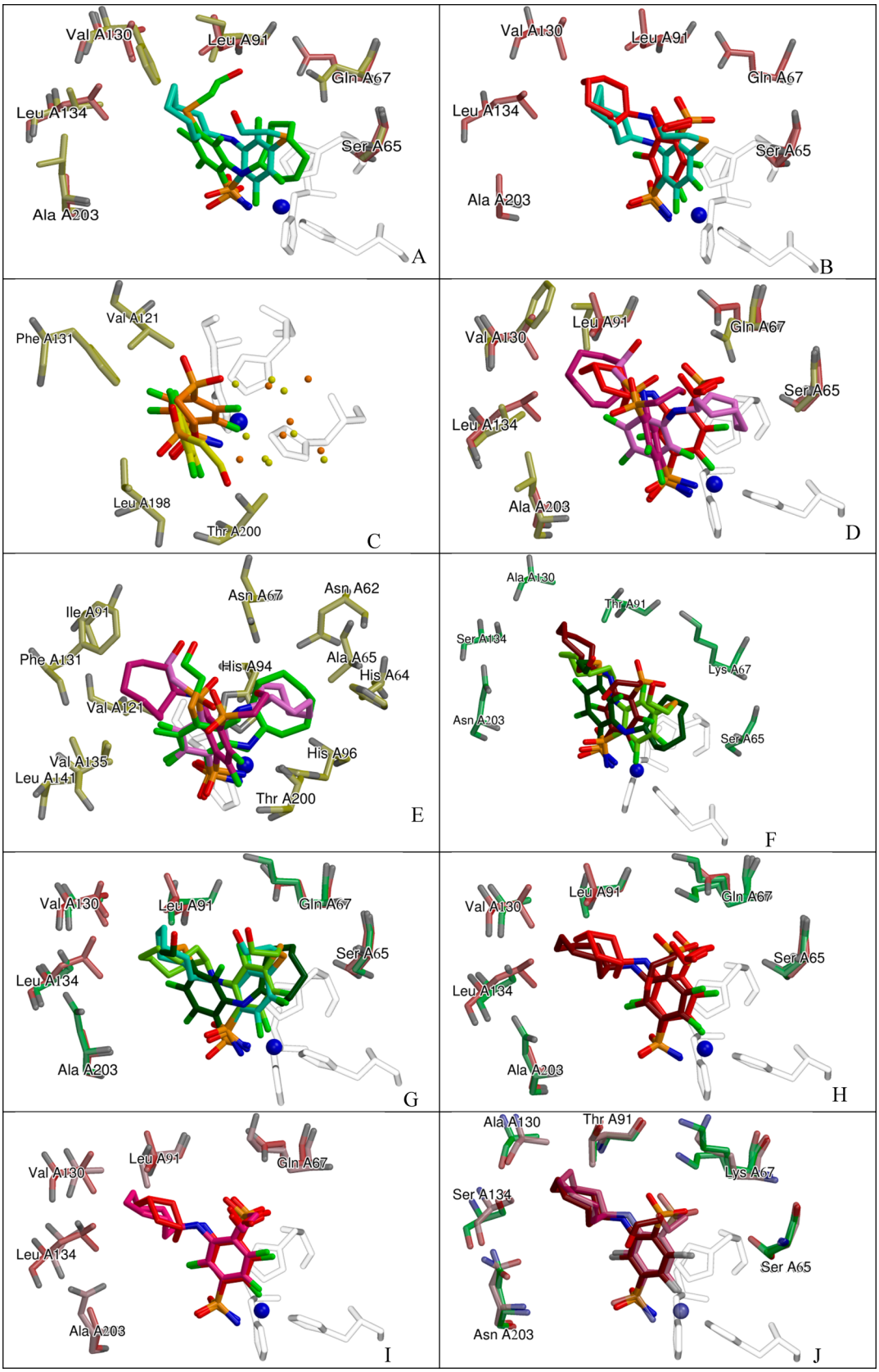

Figure 3. X-ray crystallographic structures comparing the binding modes of inhibitors bound to the active sites of CA isoforms. Inhibitors are **1** (green colors), **3** (red colors), and **5** (yellow-orange colors). The surrounding amino acids of the CA isoforms are colored: CA II, yellow; chCA IX, crystalline red; CA XII, crystalline pink; and chCA XII, crystalline green. The Zn atom is shown as a blue sphere, and the histidine residues holding the Zn are transparent. (A) Compound **1** bound to CA II (green; PDB ID 4PYX) and chCA IX (aquamarine; PDB ID 4Q06). The cyclooctyl group is pushed by Phe131 toward an opposite orientation in CA II as compared to that of Val131 in chCA IX, causing selectivity for chCA IX. Residue labeling corresponds to chCA IX. (B) Comparison of the binding modes of compounds **1** (aquamarine; PDB ID 4Q06) and **3** (red; PDB ID 4Q07)

dx.doi.org/10.1021/jm501003k | J. Med. Chem. XXXX, XXX, XXX−XXX

Figure 3. continued

bound to chCA IX. The overall position of both compounds is similar. (C) Compound **5** bound to CA II (yellow; PDB ID 4PZH) and CA XIII (orange; PDB ID 4HU1) exhibits a significantly different rotated position of the benzene ring. The active sites also contain numerous water molecules bound deeply in the active site (shown as small spheres: yellow in CA II and orange in CA XIII). The presence of these water molecules shows how much space is left unoccupied in the active site by compound **5**. These water molecules are absent in the structures with compounds **1** and **3**. (D) Compound **3** bound to CA II (there are two orientations shown in violet and violet-red; PDB ID 4PYY) and chCA IX (red; PDB ID 4Q07). The two orientations of the compound in CA II indicate the reason why the compound is bound much more weakly to CA II than to CA IX. Residue labeling corresponds to chCA IX. (E) The binding mode of compounds **1** (green; PDB ID 4PYX) and **3** (two essentially opposite orientations are shown in violet and violet-red; PDB ID 4PYY) bound to CA II. (F) Comparison of the two opposite orientations of the binding positions of **1** (dark and light green; PDB ID 4Q08) and **3** (dark red; PDB ID 4Q09) to chCA XII. (G) The positions of compound **1** bound to chCA IX (aquamarine green; PDB ID 4Q06) and chCA XII (two alternative orientations are shown in green-yellow and dark-green; PDB ID 4Q08). Residue labeling corresponds to chCA IX. (H) The comparison of positions of **3** bound to chCA IX (red; PDB ID 4Q07) and chCA XII (dark-red; PDB ID 4Q09). Residue labeling corresponds to chCA IX. (I) The positions of **3** bound to chCA IX (red; PDB ID 4Q07) and CA XII (pink; PDB ID 4Q0L) showing essentially overlapping orientations. Residue labeling corresponds to chCA IX. (J) Compound **3** bound to CA XII (deep pink; PDB ID 4Q0L) and chCA XII (dark-red; PDB ID 4Q09) in almost exactly the same orientation. Residue labeling corresponds to chCA XII.

nM. Therefore, these key amino acids caused the affinity to change significantly. First, the compound bound CA II and exhibited two oppositely facing positions. The electron density (Figure 5E) clearly could not be fit with a single pose of the ligand. The presence of two rather different positions indicates that their binding energies are quite similar and that the affinity is not high, as shown by the binding measurements.

The structures of compounds **1** and **3** bound to chCA XII and CA XII were also solved for comparison. However, their binding affinities or selectivities are significantly lower and would be less suitable to inhibit CA XII. The present compounds are thus more suitable to be developed as CA IX inhibitors rather than CA XII.

DISCUSSION

The discovery of high-affinity and -selectivity compounds toward human CA IX over all 11 remaining active human CAs has been described and reconciled both in terms of affinities and the structure of the complexes. The high affinity of the compounds was achieved by lowering the pK_a of the sulfonamide amino group by introducing electron-withdrawing fluorine atoms to the conjugated benzene ring system. Sulfonamide compounds bound and inhibited the CAs in the deprotonated form that was present in a small concentration without the presence of the withdrawing groups. For example, the pK_a of benzenesulfonamide is approximately 11, whereas for pentafluorobenzenesulfonamide, it is about 8. Therefore, the observed dissociation constant for the fluorinated sulfonamide would be approximately 1000-fold stronger due to the higher fraction of the active, deprotonated form. In compounds **1**−**5**, a strong withdrawing effect was exhibited by the fluorine atoms on the benzene ring.

The strong selectivity of the compounds was ensured by the good fit of the cyclooctyl group of both compounds to the hydrophobic pocket of CA IX. The compounds bound nicely into the pocket, with numerous hydrophobic contacts between the protein and ligand. This was not possible for CA II, where the ligand bound in an opposite orientation and made weaker contacts with the protein. Similarly, CA XII was also weakly affected by the compounds. The cyclooctyl group did not fit as in CA IX, and the compound was bound in the opposite orientation, which was significantly weaker in its binding energy. There are no structures with the remaining CAs. Therefore, we do not know the exact structural reasons why the compounds are poorer binders of these isoforms than to CA IX.

There is only one report on the crystallization of human CA IX[30] and thus inhibitor development for CA IX has been hindered by unsuccessful co-crystallization of compounds with CA IX. Therefore, a mimic of CA IX, a multiple-residue mutant in the vicinity of the active site, has been proposed and crystallized with some inhibitors.[54] Our designed chimeric CA IX (chCA IX) slightly differed from this by the selection of mutations that were supposed to better resemble the environment of the active site of CA IX. Unfortunately, such an approach cannot be considered as fully replacing the crystallization of CA IX itself. The binding data of chCA IX did not precisely resemble the binding to CA IX. However, this approach is currently the best available to enable structural visualization of the mode of binding of various CA IX inhibitors. Furthermore, this approach worked excellently for CA XII, where we determined the crystal structures of both chimeric chCA XII and CA XII itself. Both the binding data and the crystal structures confirmed that chCA XII is an excellent model of CA XII.

Several groups of CA inhibitors have shown promising selectivity in binding CA IX, such as nitroimidazole sulfonamides,[55] glycosidic sulfonamides,[56] diarylpyrazole benzenesulfonamides,[57] and technecium-containing arylsulfonamides.[58] Some nonsulfonamide compounds, namely, coumarins, were also reported to be selective CA IX inhibitors.[59−61] Furthermore, previously reported polyfluorinated compounds have shown selectivity toward CA IX.[62] However, their affinity and selectivity were relatively low because the compounds were fluorinated on the benzene ring that was not directly attached to the sulfonamide headgroup. The studies of these inhibitors were based on following only enzyme inhibition, which is often insufficient for complete characterization of the binding reaction. Furthermore, the reported selectivity was often limited and arguably of insufficient magnitude for an inhibitor against the most common CA I and CA II isoforms, i.e., the appropriate inhibition constant should be at least 1000-fold tighter than that for CA I and CA II.

It seems that in order to achieve highly selective compounds it is insufficient to have a single para substituent on the benzenesulfonamide. There are no steric constraints, and such compounds bind quite easily to most CA isoforms. Furthermore, it is insufficient to have a single ortho substituent because such compounds are also quite easily accommodated in the active site of most CAs. In order to achieve significant selectivity, it is necessary to have at least two substituents, and the most promising positions are ortho and para. Compounds that have substituents farther away from the sulfonamide group,

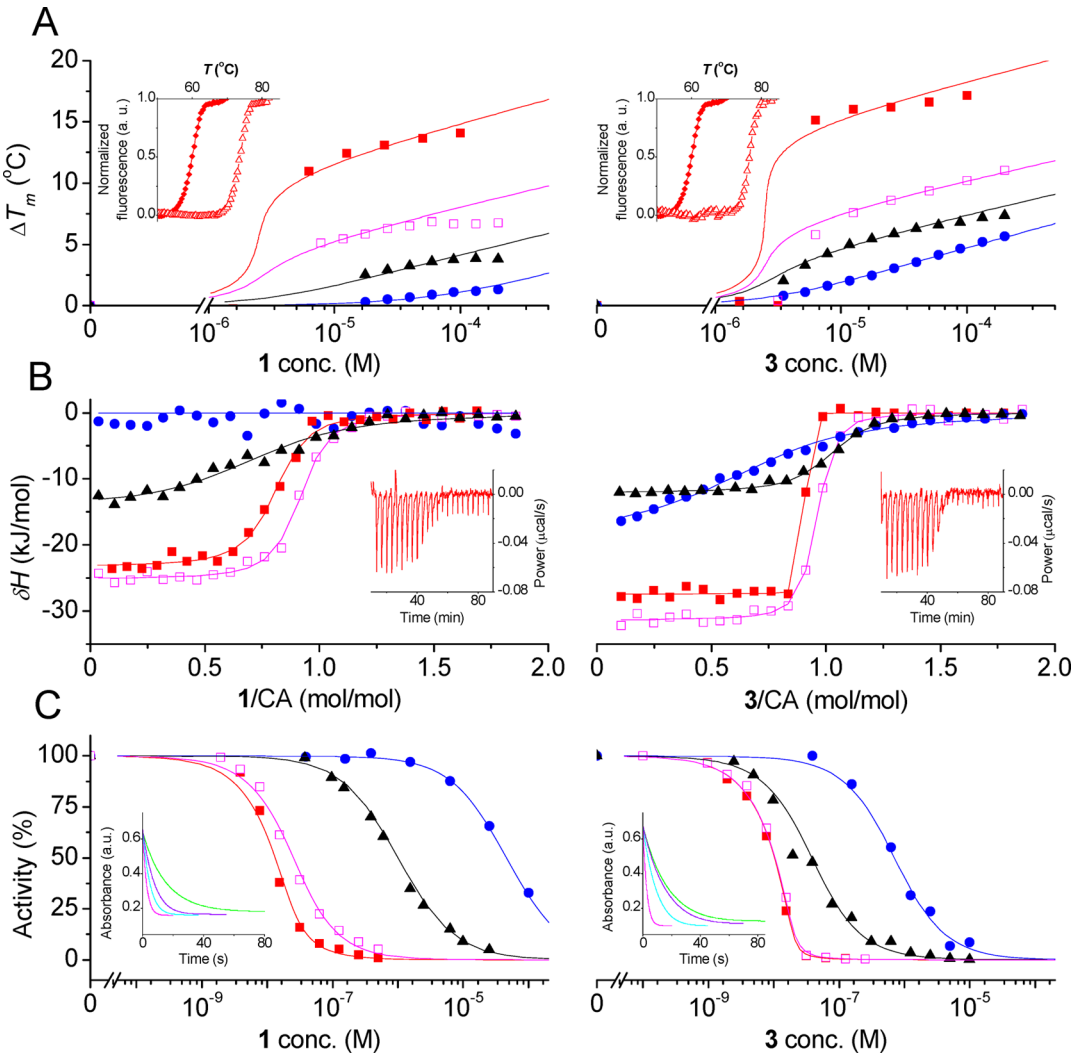

Figure 4. Compounds **1** (left) and **3** (right) binding and inhibition of CAs. (A) Binding of compounds, as determined by the thermal shift assay. Data points show the ΔT_m as a function of the total added compound concentration, and the lines are simulated according to ref 42. Red filled squares, CA IX; magenta open squares, chCA IX; black filled triangles, CA II; and blue filled circles, CA I. The largest ΔT_m shift for similar proteins corresponds to strongest binding K_d. The inset graphs show normalized raw fluorescence data as a function of temperature at zero (filled red diamonds) and 50 μM (open red triangles) of total added compound concentration. The melting midpoints correspond to the T_m. (B) Binding of the compounds, as determined by isothermal titration calorimetry. Colors and symbols for CA isoforms are the same as those in panel A. The ITC curve fitting K_d's are listed in Table 1. Insets show the raw ITC curves of the respective compound binding to CA IX. (C) The inhibition of CA isoforms, as determined by the stopped-flow kinetic CO_2 hydration assay. Colors and symbols for CA isoforms are the same as those in panel A. Data points correspond to the percent inhibition of a CA as a function of the total added compound concentration. The lines are fit according to the Morrison equation as explained in the Experimental Section. Insets show raw activity curves (drop in absorbance/pH due to acidification by the CA IX) at various added compound concentrations: magenta, 0 nM; cyan, 15.6 nM; violet, 31.3 nM; and green, spontaneous CO_2 hydration in the absence of CA IX. The CA IX concentration was 20 nM. All three methods conclusively indicate that both compounds **1** and **3** bound and inhibited CA IX significantly stronger than that for CA I and CA II. Furthermore, compound **3** bound tighter to most CA isoforms than that of **1**. However, compound **1** exhibited a greater selectivity ratio toward CA IX than that of **3**.

e.g., on consecutive rings, are expected to bear lower selectivity toward a desired isoform.

The three compounds, **1**–**3**, are good potential lead compound candidates. However, further development of the compounds may prove to be beneficial for improving affinity and selectivity. The three compounds are quite different. **2** is the most selective toward CA IX, but it has the lowest affinity (10 nM). **1** possesses 1 nM affinity toward CA IX, and, under the assumption that it would affect the other CAs in the human body only at 0.1 μM, it would affect only CA XIV in addition to CA IX. At 1 μM concentration, it would affect CAs VB, VII, XII, XIII, and XIV. However, the most abundant CAs, I and II, still would not be affected.

Compound **3** possessed an even higher affinity for CA IX, approximately 50 pM. However, this compound bound more strongly not only to the target CA IX but also to nearly all other CAs. Therefore, despite greater affinity, it seems that **3** has lower potential to be developed further as a drug candidate than that of **1**. The affinity of **3** for CA IX is extremely high. Such affinities are rarely observed for any protein–ligand system.

Several compounds have been designed and produced that strongly and selectively bind CA IX, as shown by three independent techniques. Crystal structures show the structural arrangement of the ligands in the CA IX active site, as modeled by chimeric CA IX. The compounds had to possess a highly

dx.doi.org/10.1021/jm501003k | J. Med. Chem. XXXX, XXX, XXX–XXX

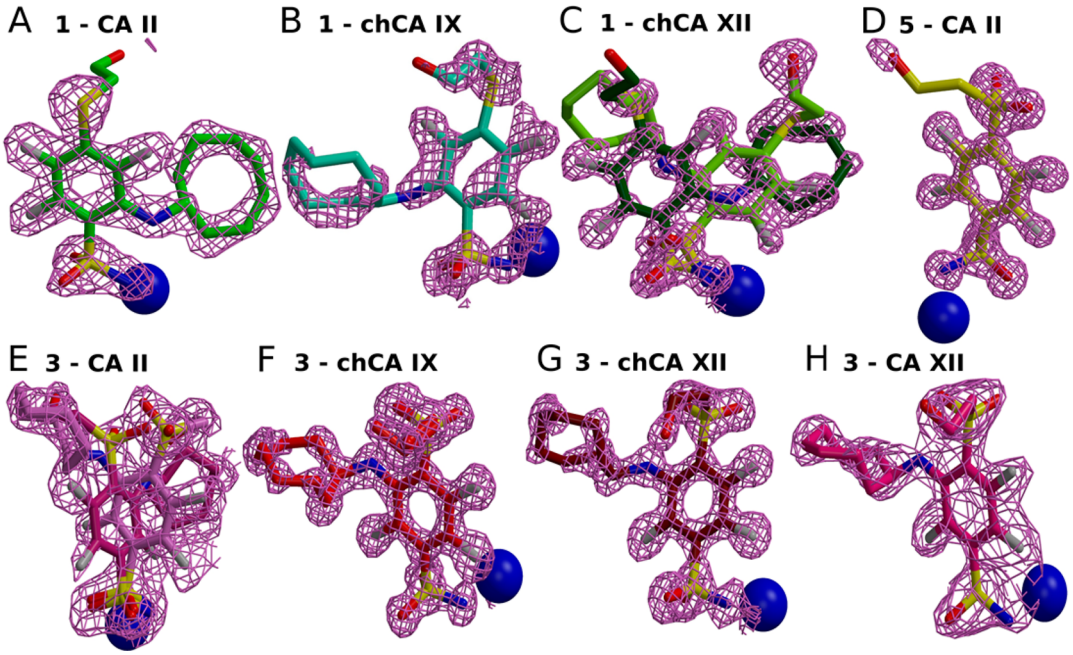

Figure 5. Electron densities of compounds bound to the active sites of CA isoforms. (A) **1** bound to CA II (PDB ID 4PYX). (B) **1** bound to chCA IX (PDB ID 4Q06). (C) **1** bound to chCA XII (two alternative positions are visible; PDB ID 4Q08). (D) **5** bound to CA II (PDB ID 4PZH). (E) **3** bound to CA II (two alternative positions are visible; PDB ID 4PYY). (F) **3** bound to chCA IX (PDB ID 4Q07). (G) **3** bound to chCA XII (PDB ID 4Q09). (H) **3** bound to CA XII (PDB ID 4Q0L). Modeled compounds are shown in the same colors as those in previous images: **1**, green; **3**, red-violet; and **5**, yellow. The catalytic Zn^{2+} is shown as a blue sphere. The electron density map $|F_{obs} - F_{calc}|$ calculated in the absence of ligand is contoured at 3.0σ (A, H) and at 2.5−2.7σ (B−G).

hydrophobic group at an ortho position relative to the aryl sulfonamide in order to exhibit high selectivity. Extremely high selectivity diminished affinity because of the strain that the compound−protein structure exhibits.

EXPERIMENTAL SECTION

Chemical Compounds. All starting materials and reagents were commercial products that were used without further purification. Melting points of the compounds were determined in open capillaries on a Thermo Scientific 9100 Series and are uncorrected. Column chromatography was performed using silica gel 60 (0.040−0.063 mm, Merck). ^{1}H and ^{13}C NMR spectra were recorded on a Varian Unity Inova spectrometer (300 and 75 MHz, respectively) with TMS as an internal standard, and proton and carbon chemical shifts are expressed in parts per million (ppm) in the indicated solvent. ^{19}F NMR spectra were recorded on a Varian Unity Inova spectrometer (282 MHz) with $CFCl_3$ as an internal standard, and fluorine chemical shifts are expressed in parts per million (ppm) in the indicated solvent. Multiplicity was defined as s (singlet), d (doublet), t (triplet), q (quartet), dd (double doublet), ddd (double double doublet), m (multiplet), br s (broad singlet), br d (broad doublet), or br t (broad triplet). TLC was performed with silica gel 60 F254 aluminum plates (Merck) and visualized with UV light. High-resolution mass spectra (HRMS) were recorded on a Dual-ESI Accurate-Mass Q-TOF LC/MS 6520 mass spectrometer (Agilent Technologies). The purity of final compounds was verified by HPLC to be >95% using the Agilent 1290 Infinity instrument with a Poroshell 120 SB-C18 (2.1 mm × 100 mm, 2.7 μm) reversed-phase column. Analytes were eluted using a linear gradient of water/methanol (20 mM ammonium formate in both phases) from 60:40 to 30:70 over 12 min, from 30:70 to 20:80 over 1 min, and then 20:80 over 5 min at a flow rate of 0.2 mL/min. UV detection was at 254 nm.

Instant JChem was used for compound structure database management, search, and prediction (Instant JChem 6.1.3, 2013, ChemAxon; http://www.chemaxon.com). The synthesis of compounds **4** and **5** has been previously described (**4** is 3c and **5** is 3d described in ref 27).

Synthesis of 2-(Cyclooctylamino)-3,5,6-trifluoro-4-[(2-hydroxyethyl)thio]benzenesulfonamide (1). A mixture of 2,3,5,6-tetrafluoro-4-[(2-hydroxyethyl)thio]benzenesulfonamide (**4**) (0.17 g, 0.55 mmol), Et_3N (0.08 mL, 0.57 mmol), DMSO (1 mL), and cyclooctylamine (0.07 g, 0.57 mmol) was stirred at 60 °C for 16 h. The mixture was then diluted with H_2O (20 mL) and extracted with EtOAc (3 × 10 mL). The combined organic phase was dried over $MgSO_4$ and evaporated under reduced pressure.

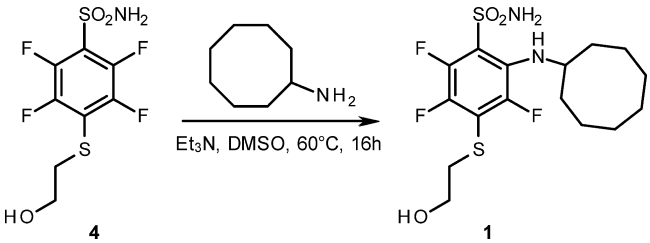

The product was purified by chromatography on a column of silica gel (0.040−0.063 mm) with EtOAc/$CHCl_3$ (1:1), R_f = 0.59. Yield: 0.15 g, 56%, mp 68−69 °C. ^{1}H NMR (300 MHz, $CDCl_3$): 1.40−1.75 (12H, m, cyclooctane), 1.80−1.95 (2H, m, cyclooctane), 2.54 (1H, br s, OH), 3.14 (2H, t, J = 5.7 Hz, $S\underline{CH_2}CH_2$), 3.74 (2H, t, J = 5.7 Hz, $SCH_2\underline{CH_2}$), 3.75−3.85 (1H, m, CH of cyclooctane, signal overlaps with signal of $SCH_2\underline{CH_2}$), 5.77 (2H, s, SO_2NH_2), 6.16 (1H, br s, NH). ^{13}C NMR (75 MHz, $CDCl_3$): 23.7 (cyclooctane), 25.8 (cyclooctane), 27.5 (cyclooctane), 33.0 (cyclooctane), 37.5 ($S\underline{CH_2}CH_2$, br t), 56.4 (CH of cyclooctane, d, J (^{19}F−^{13}C) = 11 Hz), 61.2 ($SCH_2\underline{CH_2}$), 117.9 (C1, dd, ^{1}J (^{19}F−^{13}C) = 12 Hz, ^{2}J (^{19}F−^{13}C) = 5 Hz), 118.3 (C4, t, J (^{19}F−^{13}C) = 21 Hz), 132.7 (C2, d, J (^{19}F−^{13}C) = 15 Hz), 142.1 (C5, ddd, ^{1}J (^{19}F−^{13}C) = 240 Hz, ^{2}J (^{19}F−^{13}C) = 16 Hz, ^{3}J (^{19}F−^{13}C) = 5 Hz), 145.1 (C6, ddd, ^{1}J (^{19}F−^{13}C) = 247 Hz, ^{2}J (^{19}F−^{13}C) = 16 Hz, ^{3}J (^{19}F−^{13}C) = 4 Hz), 149.1 (C3, d, J (^{19}F−^{13}C) = 243 Hz). ^{19}F NMR (282 MHz, $CDCl_3$): −124.5 (C3−F, d, J = 11 Hz), −143.0 (C5−F, dd, ^{1}J = 27 Hz, ^{2}J = 12 Hz), −149.0 (C6−F, d, J = 26 Hz). HRMS for $C_{16}H_{23}F_3N_2O_3S_2$ [$(M+H)^+$] calcd, 413.1175; found, 413.1175.

dx.doi.org/10.1021/jm501003k | J. Med. Chem. XXXX, XXX, XXX−XXX

Table 2. X-ray Crystallographic Data Collection and Refinement Statistics[a]

protein−compound	CA II−1	CA II−3	CA XII−3	CA II−5	chCA IX−1	chCA XII−1	chCA XII−3	chCA IX−3
resolution (Å)	25.22−1.80	23.76−1.75	22.09−2.00	40.82−1.06	40.74−1.15	40.66−1.07	69.03−1.20	69.86−1.15
N_{ref} (unique)	21 036	24 612	44 882	100 624	77 998	98 666	72 417	77 927
R_{merge} (outer shell)	0.127 (0.422)	0.060 (0.133)	0.068 (0.269)	0.051 (0.376)	0.063 (0.189)	0.032 (0.339)	0.042 (0.346)	0.065 (0.204)
I/σ (outer shell)	9.9 (2.3)	10.8 (6.1)	12.2 (2.8)	15.9 (4.1)	14.7 (7.2)	14.0 (3.0)	21.1 (4.4)	8.6 (4.1)
multiplicity (outer shell)	3.7 (3.7)	3.6 (3.5)	2.9 (3.0)	6.7 (6.0)	7.0 (6.7)	3.1 (2.3)	6.7 (6.4)	3.5 (3.3)
completeness (%) (outer shell)	95.1 (92.0)	99.9 (99.8)	74.5 (64.9)	93.5 (77.6)	91.4 (72.0)	93.7 (75.0)	98.8 (98.2)	92.0 (73.6)
N_{atoms}	2284	2465	8896	2527	2568	2663	2502	3103
R_{work}	0.178	0.149	0.264	0.135	0.137	0.128	0.139	0.131
R_{free}	0.23	0.2	0.328	0.162	0.169	0.156	0.178	0.159
$B_{average}$	18.949	15.231	20.194	16.549	17.922	14.474	17.478	14.353
RMS_{bonds}	0.02	0.02	0.014	0.026	0.024	0.024	0.024	0.023
RMS_{angles}	2.137	2.138	1.739	2.588	2.448	2.492	2.333	2.45
PDB ID	4PYX	4PYY	4Q0L	4PZH	4Q06	4Q08	4Q09	4Q07

[a]All datasets were collected at 100 K; test set size was 10%.

The synthesis of **2** and **3** is described in the Supporting Information.

Protein Preparation. Expression and purification of CAs I, II, VII, XII and XIII were previously described: CA I, in ref 63; CA II, in ref 43; CA VI, in ref 63; CAs VII and XIII, in ref 64; and CA XII, in ref 65. Preparation of CAs III, VA, VB, XIV, chCA IX, and chCA XII is described in the Supporting Information.

Preparation of CAs IV and IX in Mammalian Cells. The cDNAs of human CA IX and CA IV were purchased from RZPD Deutsches Ressourcenzentrum für Genomforschung GmbH (Germany). Expression of CAs IX and IV in mammalian cells was carried out using the pCEP4dS vector designed for the secretion of recombinant mammalian proteins.[66]

For the construction of pCEP4dS-CAIX plasmids, the DNA fragments, corresponding to the catalytic domain of CA IX (amino acids 38−414) were inserted into a multicloning site of the pCEP4dS vector. For the construction of the pCEP4dS-CAIV plasmid, a nucleotide sequence encoding CA IV's catalytic domain (amino acids 19−284) was inserted into a multicloning site of the pCEP4dS vector. Because of the linker located between the secretion signal and the coding sequences of the CAs, expressed CA IX had an additional 5 amino acids (DAAHM) and CA IV had an additional 8 amino acids (DAAHMKLM) located at the N terminus.

Expression of CAs IX and IV was carried out using the FreeStyle Max 293 expression system (Invitrogen, Life Technologies). FreeStyle 293-F suspension cell culture was maintained in 125−1000 mL Erlenmeyer flasks containing 30−240 mL of FreeStyle medium in a 37 °C incubator with a humidified atmosphere of 8% CO_2, on an orbital shaker platform rotating at 135 rpm. FreeStyle cells were transiently transfected with the purified pCEP4dS-CAIX or pCEP4dS-CAIV plasmids according to the manufacturer's recommendations. After 5−7 days, the cell culture was centrifuged at 6000*g* for 20 min, and the secreted recombinant proteins were purified from the supernatant using a CA-affinity column containing *p*-aminomethylbenzenesulfonamide-agarose (Sigma Life Science). The eluted CA IX was dialyzed into 50 mM sodium phosphate buffer, pH 7.0, containing 100 mM NaCl. CA IV was dialyzed into storage buffer containing 20 mM HEPES, 50 mM NaCl, pH 7.5. All purified proteins were stored at −80 °C.

Binding and Inhibition Methods. *Fluorescent Thermal Shift Assay.* FTSA experiments were performed in a Corbett Rotor-Gene 6000 (Qiagen Rotor-Gene Q) instrument using the blue channel (excitation, 365 ± 20 nm; detection, 460 ± 15 nm). Samples contained 5−10 μM protein, 0−200 μM ligand, 50 μM solvatochromic dye ANS (8-anilino-1-naphthalenesulfonate), and 50 mM phosphate buffer containing 100 mM NaCl at pH 7.0, with the final DMSO concentration at 2%. The applied heating rate was 1 °C/min. Data analysis was performed as previously described.[42]

Isothermal Titration Calorimetry. ITC experiments were performed using ITC_{200} or VP-ITC instruments (MicroCal, Inc., Northampton, MA, USA) with 5−10 μM protein solution in the cell and 50−100 μM of the ligand solution in the syringe. A typical experiment consisted of 18 or 25 injections (2 or 10 μL each) within 2 or 3 min intervals. Experiments were carried out at 37 °C in 50 mM phosphate or Tris buffer containing 100 mM NaCl at pH 7.0, with a final DMSO concentration of 2%. The affinities by ITC were determined from the slope of the ITC integrated curve, and in order for the Wiseman factor, *c*, to not exceed 1000 at 10 μM protein concentration, the K_d should be weaker than 10 nM. The dissociation constants stronger than 10 nM could not be determined by ITC and thus are shown as <10 nM in Table 1.

Stopped-Flow Kinetic CO_2 Hydration Assay. The carbon dioxide hydration activity of recombinant human CA was measured at 25 °C using an Applied Photophysics SX.18MV-R stopped-flow spectrometer according to ref 33. Reaction velocities were measured by recording the absorbance of phenol-red indicator (30 μM, λ = 557 nm). The sample consisted of carbonic anhydrase, 0−100 μM inhibitor (in ≤0.2% DMSO), and 25 mM Hepes reaction buffer containing 25 mM NaCl, pH 7.5. Saturated CO_2 solution was prepared by bubbling the gas in Milli-Q water at 25 °C for 1 h. CA concentration was chosen according to its activity: 300−500 nM, CA I; 5−20 nM, CA II; 20 nM, chCA IX; 20 nM, CA IX; 40 nM, CA XII; and 100−150 nM, CA XIII. The K_d value was determined using Morrison equation derived by Morrison and co-workers[67,68] and well-explained in the book by Copeland.[69] According to the Morrison equation, the fraction of protein bound with ligand (equivalent to the fraction of enzyme inhibited by the inhibitor) can be expressed as

$$f_b = 1 - \left([CA]_T + [I]_T + K_i^{app} - \sqrt{([CA]_T + [I]_T + K_i^{app})^2 - 4[CA]_T[I]_T}\right)/2[CA]_T$$

where $[CA]_T$ is the total concentration of the enzyme CA, $[I]_T$ is the total added inhibitor concentration, and K_i^{app} is the apparent inhibition constant equal to the protein−ligand binding constant under the assumption of one ligand/inhibitor binding to one protein molecule.

Structure Determination by X-ray Crystallography. The protein (CA) stock solutions (20 mM sodium Hepes buffer, pH 7.5, 50 mM NaCl) were concentrated by ultrafiltration to 20−60 mg/mL. Crystallization by the sitting-drop vapor-diffusion method was started by mixing equal volumes (2−3 μL) of protein solution with the corresponding reservoir buffer. Crystals were grown at 20 °C for several weeks. Crystallization buffers, space groups, and cell parameters of CA crystals are described in Supporting Information Table S1. The complexes of ligands with CA isoforms were prepared by soaking a CA

dx.doi.org/10.1021/jm501003k | J. Med. Chem. XXXX, XXX, XXX−XXX

crystal with a 0.5 mM solution of ligand prepared by mixing a 50 mM stock solution of ligand in DMSO with the corresponding reservoir solution. The soaked crystals were measured after several days.

Diffraction data from complexes of **5** with CA II and of **1** and **3** with chCA IX and chCA XII were collected at EMBL beamlines P14 and P13 at the storage ring PETRAIII (DESY, Hamburg). Data from CA II crystals soaked with **1** and **3** and **3** with CA XII were collected using a MicroMax 007 HF (Rigaku, Japan) X-ray diffractometer at the Institute of Biotechnology, Vilnius University (Lithuania). Data collection and refinement statistics are listed in Table 2.

Data sets collected at the synchrotron were processed using XDS.[70] MOSFLM[71] was used to process the data sets collected with the MicroMax 007 HF diffractometer. All structures were solved by molecular replacement using MOLREP.[72] Initial phases for the structures of CA II, chCA IX, and chCA XII were obtained using PDB ID 3HLJ. 1JD0 was used for the CA XII crystal structures. A single protein chain stripped of all ligands was used as initial model in all molecular replacement procedures. Inhibitor 3D models were created using AVOGADRO,[73] and molecule geometry description was generated using LIBREFMAC.[74] Protein models were refined and manually remodeled using REFMAC[75] and COOT.[76] All graphic representations were made with MOLSCRIPT,[77] BOBSCRIPT,[78] and RASTER3D.[79] Coordinates and structure factors have been submitted to the RCSB Protein Databank, and their accession codes are given in Table 2.

■ ASSOCIATED CONTENT

Ⓢ Supporting Information

Synthesis of compounds **2** and **3**; preparation of recombinant CA isoforms; and crystallization buffers, space groups, and cell parameters of CA crystals (Table S1). This material is available free of charge via the Internet at http://pubs.acs.org.

■ AUTHOR INFORMATION

Corresponding Author

*Tel.: +370-5-269-1884. Fax. +370-5-260-2116. E-mail: matulis@ibt.lt, daumantas.matulis@bti.vu.lt.

Notes

The authors declare no competing financial interest.

■ ACKNOWLEDGMENTS

This research was funded by a grant from the Research Council of Lithuania (LIG-09/2012). The authors are grateful for grant FP7-REGPOT-2009-1 "MoBiLi", agreement no. 245721, and COST projects TD0905 and CM0804. The authors are grateful to Prof. Claudiu T. Supuran and Daniella Wullo for teaching to perform the stopped-flow CO_2 hydration assay

■ ABBREVIATIONS USED

CA, carbonic anhydrase; CA IX, carbonic anhydrase isoform IX; chCA IX, chimeric carbonic anhydrase isoform IX; FTSA, fluorescent thermal shift assay; ITC, isothermal titration calorimetry

■ REFERENCES

(1) De Simone, G.; Supuran, C. T. Carbonic anhydrase IX: biochemical and crystallographic characterization of a novel antitumor target. *Biochim. Biophys. Acta* **2010**, *1804*, 404−409.

(2) Frost, S. C. Physiological functions of the alpha class of carbonic anhydrases. *Subcell. Biochem.* **2014**, *75*, 9−30.

(3) Pastorek, J.; Pastoreková, S.; Callebaut, I.; Mornon, J. P.; Zelník, V.; Opavský, R.; Zat'ovicová, M.; Liao, S.; Portetelle, D.; Stanbridge, E. J. Cloning and characterization of MN, a human tumor-associated protein with a domain homologous to carbonic anhydrase and a putative helix-loop-helix DNA binding segment. *Oncogene* **1994**, *9*, 2877−2888.

(4) Ivanov, S.; Liao, S. Y.; Ivanova, A.; Danilkovitch-Miagkova, A.; Tarasova, N.; Weirich, G.; Merrill, M. J.; Proescholdt, M. A.; Oldfield, E. H.; Lee, J.; Zavada, J.; Waheed, A.; Sly, W.; Lerman, M. I.; Stanbridge, E. J. Expression of hypoxia-inducible cell-surface transmembrane carbonic anhydrases in human cancer. *Am. J. Pathol.* **2001**, *158*, 905−919.

(5) McDonald, P. C.; Winum, J.-Y.; Supuran, C. T.; Dedhar, S. Recent developments in targeting carbonic anhydrase IX for cancer therapeutics. *Oncotarget* **2012**, *3*, 84−97.

(6) Pastoreková, S.; Parkkila, S.; Parkkila, A. K.; Opavský, R.; Zelník, V.; Saarnio, J.; Pastorek, J. Carbonic anhydrase IX, MN/CA IX: analysis of stomach complementary DNA sequence and expression in human and rat alimentary tracts. *Gastroenterology* **1997**, *112*, 398−408.

(7) Benej, M.; Pastorekova, S.; Pastorek, J. Carbonic anhydrase IX: regulation and role in cancer. *Subcell. Biochem.* **2014**, *75*, 199−219.

(8) Supuran, C. T. Inhibition of carbonic anhydrase IX as a novel anticancer mechanism. *World J. Clin. Oncol.* **2012**, *3*, 98−103.

(9) Tafreshi, N. K.; Lloyd, M. C.; Bui, M. M.; Gillies, R. J.; Morse, D. L. Carbonic anhydrase IX as an imaging and therapeutic target for tumors and metastases. *Subcell. Biochem.* **2014**, *75*, 221−254.

(10) Gieling, R. G.; Williams, K. J. Carbonic anhydrase IX as a target for metastatic disease. *Bioorg. Med. Chem.* **2013**, *21*, 1470−1476.

(11) Kivelä, A. J.; Knuuttila, A.; Räsänen, J.; Sihvo, E.; Salmenkivi, K.; Saarnio, J.; Pastorekova, S.; Pastorek, J.; Waheed, A.; Sly, W. S.; Salo, J. A.; Parkkila, S. Carbonic anhydrase IX in malignant pleural mesotheliomas: a potential target for anti-cancer therapy. *Bioorg. Med. Chem.* **2013**, *21*, 1483−1488.

(12) McDonald, P. C.; Dedhar, S. Carbonic anhydrase IX (CAIX) as a mediator of hypoxia-induced stress response in cancer cells. *Subcell. Biochem.* **2014**, *75*, 255−269.

(13) Sedlakova, O.; Svastova, E.; Takacova, M.; Kopacek, J.; Pastorek, J.; Pastorekova, S. Carbonic anhydrase IX, a hypoxia-induced catalytic component of the pH regulating machinery in tumors. *Front. Physiol.* **2014**, *4*, 400.

(14) Doyen, J.; Parks, S. K.; Marcié, S.; Pouysségur, J.; Chiche, J. Knock-down of hypoxia-induced carbonic anhydrases IX and XII radiosensitizes tumor cells by increasing intracellular acidosis. *Front. Oncol.* **2012**, *2*, 199.

(15) Dubois, L.; Peeters, S.; Lieuwes, N. G.; Geusens, N.; Thiry, A.; Wigfield, S.; Carta, F.; McIntyre, A.; Scozzafava, A.; Dogné, J.-M.; Supuran, C. T.; Harris, A. L.; Masereel, B.; Lambin, P. Specific inhibition of carbonic anhydrase IX activity enhances the in vivo therapeutic effect of tumor irradiation. *Radiother. Oncol.* **2011**, *99*, 424−431.

(16) Dubois, L.; Peeters, S. G. J. A.; van Kuijk, S. J. A.; Yaromina, A.; Lieuwes, N. G.; Saraya, R.; Biemans, R.; Rami, M.; Parvathaneni, N. K.; Vullo, D.; Vooijs, M.; Supuran, C. T.; Winum, J. Y.; Lambin, P. Targeting carbonic anhydrase IX by nitroimidazole based sulfamides enhances the therapeutic effect of tumor irradiation: a new concept of dual targeting drugs. *Radiother. Oncol.* **2013**, *108*, 523−528.

(17) Ilardi, G.; Zambrano, N.; Merolla, F.; Siano, M.; Varricchio, S.; Vecchione, M.; De Rosa, G.; Mascolo, M.; Staibano, S. Histopathological determinants of tumor resistance: a special look to the immunohistochemical expression of carbonic anhydrase IX in human cancers. *Curr. Med. Chem.* **2014**, *21*, 1569−1582.

(18) Aspatwar, A.; Tolvanen, M. E. E.; Ortutay, C.; Parkkila, S. Carbonic anhydrase related proteins: molecular biology and evolution. *Subcell. Biochem.* **2014**, *75*, 135−156.

(19) Supuran, C. T. Carbonic anhydrases—an overview. *Curr. Pharm. Des.* **2008**, *14*, 603−14.

(20) Aggarwal, M.; Boone, C. D.; Kondeti, B.; McKenna, R. Structural annotation of human carbonic anhydrases. *J. Enzyme Inhib. Med. Chem.* **2013**, *28*, 267−277.

(21) De Simone, G.; Alterio, V.; Supuran, C. T. Exploiting the hydrophobic and hydrophilic binding sites for designing carbonic anhydrase inhibitors. *Expert Opin. Drug Discovery* **2013**, *8*, 793−810.

(22) Innocenti, A.; Pastorekova, S.; Pastorek, J.; Scozzafava, A.; De Simone, G.; Supuran, C. T. The proteoglycan region of the tumor-associated carbonic anhydrase isoform IX acts as an intrinsic buffer

optimizing CO_2 hydration at acidic pH values characteristic of solid tumors. *Bioorg. Med. Chem. Lett.* **2009**, *19*, 5825−5828.
(23) Alterio, V.; Di Fiore, A.; D'Ambrosio, K.; Supuran, C. T.; De Simone, G. Multiple binding modes of inhibitors to carbonic anhydrases: how to design specific drugs targeting 15 different isoforms? *Chem. Rev.* **2012**, *112*, 4421−4468.
(24) Krishnamurthy, V. M.; Kaufman, G. K.; Urbach, A. R.; Gitlin, I.; Gudiksen, K. L.; Weibel, D. B.; Whitesides, G. M. Carbonic anhydrase as a model for biophysical and physical-organic studies of proteins and protein−ligand binding. *Chem. Rev.* **2008**, *108*, 946−1051.
(25) Miller, W. H.; Dessert, A. M.; Roblin, R. O. Heterocyclic sulfonamides as carbonic anhydrase inhibitors. *J. Am. Chem. Soc.* **1950**, *72*, 4893−4896.
(26) Swenson, E. R. Safety of carbonic anhydrase inhibitors. *Expert Opin. Drug Saf.* **2014**, *13*, 459−472.
(27) Dudutienė, V.; Zubrienė, A.; Smirnov, A.; Gylytė, J.; Timm, D.; Manakova, E.; Gražulis, S.; Matulis, D. 4-Substituted-2,3,5,6-tetrafluorobenzenesulfonamides as inhibitors of carbonic anhydrases I, II, VII, XII, and XIII. *Bioorg. Med. Chem.* **2013**, *21*, 2093−2106.
(28) Krishnamurthy, V. M.; Bohall, B. R.; Kim, C.-Y.; Moustakas, D. T.; Christianson, D. W.; Whitesides, G. M. Thermodynamic parameters for the association of fluorinated benzenesulfonamides with bovine carbonic anhydrase II. *Chem.−Asian J.* **2007**, *2*, 94−105.
(29) Winum, J. Y.; Innocenti, A.; Vullo, D.; Montero, J. L.; Supuran, C. T. Carbonic anhydrase inhibitors; fluorinated phenyl sulfamates show strong inhibitory activity and selectivity for the inhibition of the tumor-associated isozymes IX and XII over the cytosolic ones I and II. *Bioorg. Med. Chem. Lett.* **2009**, *19*, 5082−5085.
(30) Alterio, V.; Hilvo, M.; Di Fiore, A.; Supuran, C. T.; Pan, P.; Parkkila, S.; Scaloni, A.; Pastorek, J.; Pastorekova, S.; Pedone, C.; Scozzafava, A.; Monti, S. M.; De Simone, G. Crystal structure of the catalytic domain of the tumor-associated human carbonic anhydrase IX. *Proc. Natl. Acad. Sci. U.S.A.* **2009**, *106*, 16233−16238.
(31) Hilvo, M.; Baranauskienė, L.; Salzano, A. M.; Scaloni, A.; Matulis, D.; Innocenti, A.; Scozzafava, A.; Monti, S. M.; Di Fiore, A.; De Simone, G.; Lindfors, M.; Janis, J.; Valjakka, J.; Pastorekova, S.; Pastorek, J.; Kulomaa, M. S.; Nordlund, H. R.; Supuran, C. T.; Parkkila, S. Biochemical characterization of CA IX, one of the most active carbonic anhydrase isozymes. *J. Biol. Chem.* **2008**, *283*, 27799−27809.
(32) Biswas, S.; McKenna, R.; Supuran, C. T. Effect of incorporating a thiophene tail in the scaffold of acetazolamide on the inhibition of human carbonic anhydrase isoforms I, II, IX and XII. *Bioorg. Med. Chem. Lett.* **2013**, *23*, 5646−5649.
(33) Khalifah, R. G. The carbon dioxide hydration activity of carbonic anhydrase. I. Stop-flow kinetic studies on the native human isoenzymes B and C. *J. Biol. Chem.* **1971**, *246*, 2561−2573.
(34) McKenna, R.; Supuran, C. T. Carbonic anhydrase inhibitors drug design. *Subcell. Biochem.* **2014**, *75*, 291−323.
(35) Biela, A.; Betz, M.; Heine, A.; Klebe, G. Water makes the difference: rearrangement of water solvation layer triggers non-additivity of functional group contributions in protein−ligand binding. *ChemMedChem.* **2012**, *7*, 1423−1434.
(36) Holdgate, G. A. Making cool drugs hot: isothermal titration calorimetry as a tool to study binding energetics. *BioTechniques* **2001**, *31*, 164−184.
(37) Ladbury, J. E. Isothermal titration calorimetry: application to structure-based drug design. *Thermochim. Acta* **2001**, *380*, 209−215.
(38) Wiseman, T.; Williston, S.; Brandts, J. F.; Lin, L. N. Rapid measurement of binding constants and heats of binding using a new titration calorimeter. *Anal. Biochem.* **1989**, *179*, 131−137.
(39) Babon, J. J. Quantitative analysis of JAK binding using isothermal titration calorimetry and surface plasmon resonance. *Methods Mol. Biol.* **2013**, *967*, 57−67.
(40) Jecklin, M. C.; Schauer, S.; Dumelin, C. E.; Zenobi, R. Label-free determination of protein-ligand binding constants using mass spectrometry and validation using surface plasmon resonance and isothermal titration calorimetry. *J. Mol. Recognit.* **2009**, *22*, 319−329.
(41) Rogez-Florent, T.; Duhamel, L.; Goossens, L.; Six, P.; Drucbert, A.-S.; Depreux, P.; Danzé, P.-M.; Landy, D.; Goossens, J.-F.; Foulon, C. Label-free characterization of carbonic anhydrase-novel inhibitor interactions using surface plasmon resonance, isothermal titration calorimetry and fluorescence-based thermal shift assays. *J. Mol. Recognit.* **2014**, *27*, 46−56.
(42) Baranauskienė, L.; Hilvo, M.; Matulienė, J.; Golovenko, D.; Manakova, E.; Dudutienė, V.; Michailovienė, V.; Torresan, J.; Jachno, J.; Parkkila, S.; Maresca, A.; Supuran, C. T.; Gražulis, S.; Matulis, D. Inhibition and binding studies of carbonic anhydrase isozymes I, II and IX with benzimidazo[1,2-*c*][1,2,3]thiadiazole-7-sulphonamides. *J. Enzyme Inhib. Med. Chem.* **2010**, *25*, 863−870.
(43) Cimmperman, P.; Baranauskienė, L.; Jachimovičiūtė, S.; Jachno, J.; Torresan, J.; Michailovienė, V.; Matulienė, J.; Sereikaitė, J.; Bumelis, V.; Matulis, D. A quantitative model of thermal stabilization and destabilization of proteins by ligands. *Biophys. J.* **2008**, *95*, 3222−3231.
(44) Cimmperman, P.; Matulis, D. Protein thermal denaturation measurements via a fluorescent dye. In *Biophysical Approaches Determining Ligand Binding to Biomolecular Targets*; Alberto Podjarny, A. D., Kieffer, B., Eds.; RSC Publishing: Cambridge, 2011; pp 247−274.
(45) Zubrienė, A.; Čapkauskaitė, E.; Gylytė, J.; Kišonaitė, M.; Tumkevičius, S.; Matulis, D. Benzenesulfonamides with benzimidazole moieties as inhibitors of carbonic anhydrases I, II, VII, XII and XIII. *J. Enzyme Inhib. Med. Chem.* **2014**, *29*, 124−131.
(46) Zubrienė, A.; Kazlauskas, E.; Baranauskienė, L.; Petrauskas, V.; Matulis, D. Isothermal titration calorimetry and thermal shift assay in drug design. *Eur. Pharm. Rev.* **2011**, *16*, 56−59.
(47) Niesen, F. H.; Berglund, H.; Vedadi, M. The use of differential scanning fluorimetry to detect ligand interactions that promote protein stability. *Nat. Protoc.* **2007**, *2*, 2212−2221.
(48) Cummings, M. D.; Farnum, M. A.; Nelen, M. I. Universal screening methods and applications of ThermoFluor. *J. Biomol. Screen.* **2006**, *11*, 854−863.
(49) Klinger, A. L.; McComsey, D. F.; Smith-Swintosky, V.; Shank, R. P.; Maryanoff, B. E. Inhibition of carbonic anhydrase-II by sulfamate and sulfamide groups: an investigation involving direct thermodynamic binding measurements. *J. Med. Chem.* **2006**, *49*, 3496−500.
(50) Matulis, D.; Kranz, J. K.; Salemme, F. R.; Todd, M. J. Thermodynamic stability of carbonic anhydrase: measurements of binding affinity and stoichiometry using ThermoFluor. *Biochemistry* **2005**, *44*, 5258−5266.
(51) Mezzasalma, T. M.; Kranz, J. K.; Chan, W.; Struble, G. T.; Schalk-Hihi, C.; Deckman, I. C.; Springer, B. A.; Todd, M. J. Enhancing recombinant protein quality and yield by protein stability profiling. *J. Biomol. Screening* **2007**, *12*, 418−428.
(52) Nettleship, J. E.; Brown, J.; Groves, M. R.; Geerlof, A. Methods for protein characterization by mass spectrometry, thermal shift (ThermoFluor) assay, and multiangle or static light scattering. *Methods Mol. Biol.* **2008**, *426*, 299−318.
(53) Pantoliano, M. W.; Petrella, E. C.; Kwasnoski, J. D.; Lobanov, V. S.; Myslik, J.; Graf, E.; Carver, T.; Asel, E.; Springer, B. A.; Lane, P.; Salemme, F. R. High-density miniaturized thermal shift assays as a general strategy for drug discovery. *J. Biomol. Screening* **2001**, *6*, 429−440.
(54) Pinard, M. A.; Boone, C. D.; Rife, B. D.; Supuran, C. T.; McKenna, R. Structural study of interaction between brinzolamide and dorzolamide inhibition of human carbonic anhydrases. *Bioorg. Med. Chem.* **2013**, *21*, 7210−7215.
(55) Rami, M.; Dubois, L.; Parvathaneni, N.-K.; Alterio, V.; van Kuijk, S. J. A.; Monti, S. M.; Lambin, P.; De Simone, G.; Supuran, C. T.; Winum, J.-Y. Hypoxia-targeting carbonic anhydrase IX inhibitors by a new series of nitroimidazole-sulfonamides/sulfamides/sulfamates. *J. Med. Chem.* **2013**, *56*, 8512−8520.
(56) Winum, J.-Y.; Colinas, P. A.; Supuran, C. T. Glycosidic carbonic anhydrase IX inhibitors: a sweet approach against cancer. *Bioorg. Med. Chem.* **2013**, *21*, 1419−1426.
(57) Rogez-Florent, T.; Meignan, S.; Foulon, C.; Six, P.; Gros, A.; Bal-Mahieu, C.; Supuran, C. T.; Scozzafava, A.; Frédérick, R.;

Masereel, B.; Depreux, P.; Lansiaux, A.; Goossens, J.-F.; Gluszok, S.; Goossens, L. New selective carbonic anhydrase IX inhibitors: synthesis and pharmacological evaluation of diarylpyrazole-benzenesulfonamides. *Bioorg. Med. Chem.* **2013**, *21*, 1451−1464.
(58) Can, D.; Spingler, B.; Schmutz, P.; Mendes, F.; Raposinho, P.; Fernandes, C.; Carta, F.; Innocenti, A.; Santos, I.; Supuran, C. T.; Alberto, R. [(Cp-R)M(CO)3] (M=Re or 99mTc) Arylsulfonamide, arylsulfamide, and arylsulfamate conjugates for selective targeting of human carbonic anhydrase IX. *Angew. Chem., Int. Ed.* **2012**, *51*, 3354−3357.
(59) Carradori, S. Selective carbonic anhydrase IX inhibitors based on coumarin scaffold as promising antimetastatic agents: WO2012070024. *Expert Opin. Ther. Pat.* **2013**, *23*, 751−756.
(60) Sharma, A.; Tiwari, M.; Supuran, C. T. Novel coumarins and benzocoumarins acting as isoform-selective inhibitors against the tumor-associated carbonic anhydrase IX. *J. Enzyme Inhib. Med. Chem.* **2014**, *29*, 292−296.
(61) Touisni, N.; Maresca, A.; McDonald, P. C.; Lou, Y.; Scozzafava, A.; Dedhar, S.; Winum, J.-Y.; Supuran, C. T. Glycosyl coumarin carbonic anhydrase IX and XII inhibitors strongly attenuate the growth of primary breast tumors. *J. Med. Chem.* **2011**, *54*, 8271−8277.
(62) Pastorekova, S.; Vullo, D.; Casini, A.; Scozzafava, A.; Pastorek, J.; Nishimori, I.; Supuran, C. T. Carbonic anhydrase inhibitors: inhibition of the tumor-associated isozymes IX and XII with polyfluorinated aromatic/heterocyclic sulfonamides. *J. Enzyme Inhib. Med. Chem.* **2005**, *20*, 211−217.
(63) Čapkauskaitė, E.; Zubrienė, A.; Smirnov, A.; Torresan, J.; Kišonaitė, M.; Kazokaitė, J.; Gylytė, J.; Michailovienė, V.; Jogaitė, V.; Manakova, E.; Gražulis, S.; Tumkevičius, S.; Matulis, D. Benzenesulfonamides with pyrimidine moiety as inhibitors of human carbonic anhydrases I, II, VI, VII, XII, and XIII. *Bioorg. Med. Chem.* **2013**, *21*, 6937−6947.
(64) Sūdžius, J.; Baranauskienė, L.; Golovenko, D.; Matulienė, J.; Michailovienė, V.; Torresan, J.; Jachno, J.; Sukackaitė, R.; Manakova, E.; Gražulis, S.; Tumkevičius, S.; Matulis, D. 4-[*N*-(Substituted 4-pyrimidinyl)amino]benzenesulfonamides as inhibitors of carbonic anhydrase isozymes I, II, VII, and XIII. *Bioorg. Med. Chem.* **2010**, *18*, 7413−7421.
(65) Jogaitė, V.; Zubrienė, A.; Michailovienė, V.; Gylytė, J.; Morkūnaitė, V.; Matulis, D. Characterization of human carbonic anhydrase XII stability and inhibitor binding. *Bioorg. Med. Chem.* **2013**, *21*, 1431−1436.
(66) Dekaminavičiūtė, D.; Kairys, V.; Žilnytė, M.; Petrikaitė, V.; Jogaitė, V.; Matulienė, J.; Gudlevičienė, Ž.; Vullo, D.; Supuran, C. T.; Žvirblienė, A. Monoclonal antibodies raised against 167−180 aa sequence of human carbonic anhydrase XII inhibit its enzymatic activity. *J. Enzyme Inhib. Med. Chem.* **2014**, DOI: 10.3109/14756366.2013.856424.
(67) Morrison, J. F. Kinetics of the reversible inhibition of enzyme-catalysed reactions by tight-binding inhibitors. *Biochim. Biophys. Acta* **1969**, *185*, 269−286.
(68) Williams, J. W.; Morrison, J. F.; Duggleby, R. G. Methotrexate, a high-affinity pseudosubstrate of dihydrofolate reductase. *Biochemistry* **1979**, *18*, 2567−2573.
(69) Copeland, R. A. *Evaluation of Enzyme Inhibitors in Drug Discovery: A Guide for Medicinal Chemists and Pharmacologists*; John Wiley & Sons, Inc.: Hoboken, NJ, 2013.
(70) Kabsch, W. Integration, scaling, space-group assignment and post-refinement. *Acta Crystallogr., Sect. D: Biol. Crystallogr.* **2010**, *66*, 133−144.
(71) Leslie, A. G. W. The integration of macromolecular diffraction data. *Acta Crystallogr., Sect. D: Biol. Crystallogr.* **2006**, *62*, 48−57.
(72) Vagin, A.; Teplyakov, A. MOLREP: an automated program for molecular replacement. *J. Appl. Crystallogr.* **1997**, *30*, 1022−1025.
(73) Avogadro: an open-source molecular builder and visualization tool, version 1.0.0, 2009; http://avogadro.openmolecules.net/.
(74) Vagin, A. A.; Steiner, R. A.; Lebedev, A. A.; Potterton, L.; McNicholas, S.; Long, F.; Murshudov, G. N. REFMAC5 dictionary: organization of prior chemical knowledge and guidelines for its use. *Acta Crystallogr., Sect. D: Biol. Crystallogr.* **2004**, *60*, 2184−2195.
(75) Murshudov, G. N.; Vagin, A. A.; Dodson, E. J. Refinement of macromolecular structures by the maximum-likelihood method. *Acta Crystallogr., Sect. D: Biol. Crystallogr.* **1997**, *53*, 240−55.
(76) Emsley, P.; Cowtan, K. Coot: model-building tools for molecular graphics. *Acta Crystallogr., Sect. D: Biol. Crystallogr.* **2004**, *60*, 2126−2132.
(77) Kraulis, P. J. MOLSCRIPT: a program to produce both detailed and schematic plots of protein structures. *J. Appl. Crystallogr.* **1991**, *24*, 946−950.
(78) Esnouf, R. M. Further additions to MolScript version 1.4, including reading and contouring of electron-density maps. *Acta Crystallogr., Sect. D: Biol. Crystallogr.* **1999**, *55*, 938−940.
(79) Merritt, E. A.; Bacon, D. J. Raster3D: photorealistic molecular graphics. *Methods Enzymol.* **1997**, *277*, 505−524.